Synthesis and characterization of $La_{0.825}Sr_{0.175}MnO_3$ nanowires

2005 J. Phys.: Condens. Matter 17 L467

(http://iopscience.iop.org/0953-8984/17/44/L02)

INSTITUTE OF PHYSICS PUBLISHING JOURNAL OF PHYSICS: CONDENSED MATTER

J. Phys.: Condens. Matter **17** (2005) L467–L475 doi:10.1088/0953-8984/17/44/L02

LETTER TO THE EDITOR

Synthesis and characterization of $La_{0.825}Sr_{0.175}MnO_3$ nanowires

F Chen[1,2], H W Liu[1], K F Wang[1], H Yu[1], S Dong[1], X Y Chen[1], X P Jiang[2], Z F Ren[1,3] and J-M Liu[1,4,5]

[1] Nanjing National Laboratory of Microstructures, Nanjing University, Nanjing 210093, People's Republic of China
[2] Department of Materials Sciences, Jingdezhen Ceramic Institute, Jiangxi, People's Republic of China
[3] Department of Physics, Boston College, Chestnut Hill, MA 02467, USA
[4] International Center for Materials Physics, Chinese Academy of Sciences, Shenyang, People's Republic of China

E-mail: liujm@nju.edu.cn

Received 3 August 2005, in final form 23 September 2005
Published 14 October 2005
Online at stacks.iop.org/JPhysCM/17/L467

Abstract

Perovskite oxide $La_{0.825}Sr_{0.175}MnO_3$ (LSMO) nanowires are synthesized using the anodized alumina oxide template technique and the characterization of the microstructure, magnetic and photoluminescence properties is performed. The as-prepared LSMO nanowires 50 nm in diameter and tens of microns in length exhibit polycrystalline perovskite structure. The magnetic measurement reveals the competition between antiferromagnetic ordering and spin glass state as ground state in the nanowires, which is different from the magnetic behaviours of bulk ceramic and single crystals. The photoluminescence (PL) spectroscopy demonstrates strong and broadband emissions with two luminescent peaks at 400 and 420 nm, respectively, which are believed to originate from the self-trapped excitons, oxygen vacancies and surface states, respectively.

Nanoscale one-dimensional structures have attracted much interest because of their novel magnetic, electronic and optical properties as a result of their low dimensionality and quantum confinement effect. In addition to the well known examples of carbon nanotubes, ZnO nanobelts and so on, nanowires of complicated perovskite functional oxides such as ferroelectric $BaTiO_3$ and $Pb(Zr, Ti)O_3$, as well as colossal magnetoresistance (CMR) manganites, have been synthesized [1–5]. Among the various methods used for fabrication of nanowires, the template synthesis method has been playing an important role in the fabrication of many kinds of nanowires and nanotubes for their interesting and useful features. Possible templates include nuclear track-etched polycarbonate membranes, nanochannel array glasses,

[5] Author to whom any correspondence should be addressed.

mesoporous channel hosts, and self-ordered anodized aluminium oxide (AAO) films. It has been found that the AAO template with diameters ranging from below 10 to 200 nm is stable at high temperature and in organic solvents, and that the pore channels in AAO films are uniform, parallel, and perpendicular to the membrane surface. This makes AAO films ideal templates for the synthesis of oxide nanowire [6].

The CMR manganites with the general formula $RE_{1-x}AE_xMnO_3$ (where RE and AE are rare and alkaline earth ions, respectively) have unusual magnetic and electronic properties. This effect is attracting considerable interest from both fundamental and practical points of view. Recently, the fabrication of $La_{0.67}Ca_{0.33}MnO_3$ ordered arrayed nanowires was done and it was found that the reported ferromagnetic transition point T_c is higher than that for single crystals [5]. The growth of $La_{0.67}Sr_{0.33}MnO_3$ oriented nanowires within the pores of AAO templates was also reported [7], although not much characterization of the physical properties was presented. These works allow us to expect significant change of the properties of CMR manganites induced by the low dimensionality of nanowire. Here, it should be mentioned that $La_{1-x}Sr_xMnO_3$, a material of the large bandwidth subset of manganese oxides, is considered as the most representative double-exchange (DE) system. Here one assumes that the doped holes reside on Mn sites, although some measurements show that the doped holes reside on oxygen sites rather than on Mn sites [8–10]. In order to achieve a large CMR effect, the insulating phase is as important as the metallic phase, and the region of the most interest should be the boundary at which metallic and insulating phases coexist and/or ferromagnetic (FM) and antiferromagnetic (AFM) phases co-appear as the ground state. Thus, it is possible for the metallic percolative transitions to take place under a very low external magnetic field.

For $La_{1-x}Sr_xMnO_3$, it was shown that the CMR effect is maximized at the compositional point separating the insulating from metallic states at low temperature (T), namely $x = 0.175$ [10]. This point represents the phase boundary at low T, and it is nowadays well accepted that the ground state at low T is a phase separated state in which the FM state and AFM charge-order state coexist [8], indicating a comparable competition between the two phases as the ground state. This allows us to predict that significant fluctuations of the magnetic property for the materials ($x = 0.175$) in nanowire form, induced by the low dimensionality, may be possible, and also of interest. Although various forms like ceramics and thin films of $La_{0.825}Sr_{0.175}MnO_3$ (LSMO) were synthesized [10, 11], preparation of LSMO quasi-one-dimensional nanowires has not yet been reported.

On the other hand, the photoemission performance of CMR manganites has been the subject of intensive research. The k-dependent spectral weight at the Fermi level was observed extensively using the angle-resolved photoemission spectroscopy (ARPES) [12]. However, few reports about the photoluminescence (PL) behaviours of CMR manganites were found, and in particular no data on the photoemission of low-dimensional manganite nanowires are available. In this letter, we report the synthesis of LSMO ($x = 0.175$) nanowires by the AAO template technique and characterization of the magnetic and PL properties.

The AAO templates were prepared by means of anodization and the LSMO nanowires were synthesized by the sol–gel method utilizing the AAO templates. The porous AAO templates were fabricated by anodizing pure aluminium foil (purity 99.5%) in a sulfuric acid solution using a two-step process. Aluminium foil was annealed at 500 °C for 4 h to form texture, then degreased in acetone. After 2 h anodization at 27 V in 0.4 M sulfuric acid solution at 0 °C, the anodic oxide layer was removed in a mixture of 0.4 M H_3PO_4 and 0.2 M H_2CrO_4. The specimen was anodized again for 4 h under the same conditions as step one. Then the Al layer was removed in a saturated $CuCl_2$ solution. The pore diameter was adjusted in 6 wt% H_3PO_4 solution at 30 °C for 30 min, forming a through-hole membrane with pore diameters of about 50 nm.

The LSMO precursor was prepared by dissolving a stoichiometric ratio of lanthanum nitrate [$La(NO_3)_3 \cdot 6H_2O$], manganese acetate [$Mn(CH_3COO)_2 \cdot 4H_2O$] and strontium acetate [$Sr(CH_3COO)_2$] in water and acetic acid, respectively. About 3 ml of acetyl acetone ($C_5H_8O_2$) was added to the solution to stabilize the LSMO solution. The concentration of the final solution was adjusted to 0.3 M and the pH value of 4–5. The AAO templates were dipped in the precursor solution for 12 h and then subsequently the surfaces were cleaned. Heating the templates containing the precursor in air at 700 °C for 30 min using a thermal annealing furnace was sufficient to obtain the desired perovskite phase of LSMO. This annealing temperature is only half of the sintering temperature for LSMO powders using the solid state reaction route (1450 °C). The morphology and structure of the LSMO nanowires were investigated using x-ray diffraction (XRD), field-emission scanning electron microscopy (FESEM), and high-resolution transmission electron microscopy (HRTEM). The magnetic properties of the LSMO nanowires were characterized by a superconductive quantum interference device (SQUID). At room temperature, the PL spectra of the nanowire sample were measured using a visible–ultraviolet spectrophotometer.

Figure 1(a) shows the SEM images of the AAO templates. The diameters of the pores and the thicknesses of the AAO templates are about 50 nm and tens of microns, respectively. The SEM observation of the as-prepared nanowires was done along the cross section and compared with the empty AAO templates. It was evident that the pores of the membrane were almost completely filled with nanowires. Figure 1(b) is the corresponding SEM image of the free-standing LSMO nanowires deposited on a silicon substrate after etching away the alumina using a 4 M NaOH solution. These nanowires have almost identical diameters. The XRD spectrum of the LSMO nanowires after dissolving away the surface alumina is shown in figure 1(c). The reflection peaks are clearly distinguishable, and can be indexed as reflections from the perovskite LSMO structures.

The microstructure of the nanowires is further analysed using HRTEM. The HRTEM specimens were prepared by dissolving the AAO templates filled with nanowires in the 4 M NaOH solution, then dispersing the LSMO nanowires in ethyl ethanol by ultrasonic vibration, and finally dropping the solution onto carbon films on copper grids. Figure 2(a) shows the TEM image of a single LSMO nanowire, about 50 nm in diameter and tens of microns in length, in good agreement with the pore diameters of the AAO templates. The perovskite structure was further confirmed by the atomic level image shown in figure 2(b), where the well recognized lattice of 3.8 Å corresponds to the {110} atomic plane of LSMO, matching with the XRD results. The insets in figures 2(a) and (b) reveal the polycrystalline structure nature of the LSMO nanowires.

For the SQUID measurement of the magnetic behaviours, we collect the nanowires in powder form after dissolving the AAO templates. However, the nanowires in the samples for magnetic measurement are randomly aligned and the measured data represent an average over all orientations of the nanowires. It is well known that LSMO ceramics offer a FM transition at about 270 K, below which there exists a competition between the FM and AFM states due to the phase separation (PS), while the FM state is dominant and the AFM state is partially restrained [10]. In figure 3(a) is plotted the T dependent magnetization M measured under a magnetic field of 100 Oe in a heating path after the sample was zero-field cooled to 5 K. It is observed that a weak AFM transition takes place at $T \sim 150$ K, and subsequently a superparamagnet (SPM) transition characterized by the gradually increasing magnetization appears upon further decreasing of T down to 25 K. This demonstrates that in the LSMO nanowires the AFM state as the ground state is dominant while the FM state is restrained to some extent. Here, what should be mentioned is that the electronic PS is constrained to be at nanometre scale because the coulomb interaction restricts the domains size of the two

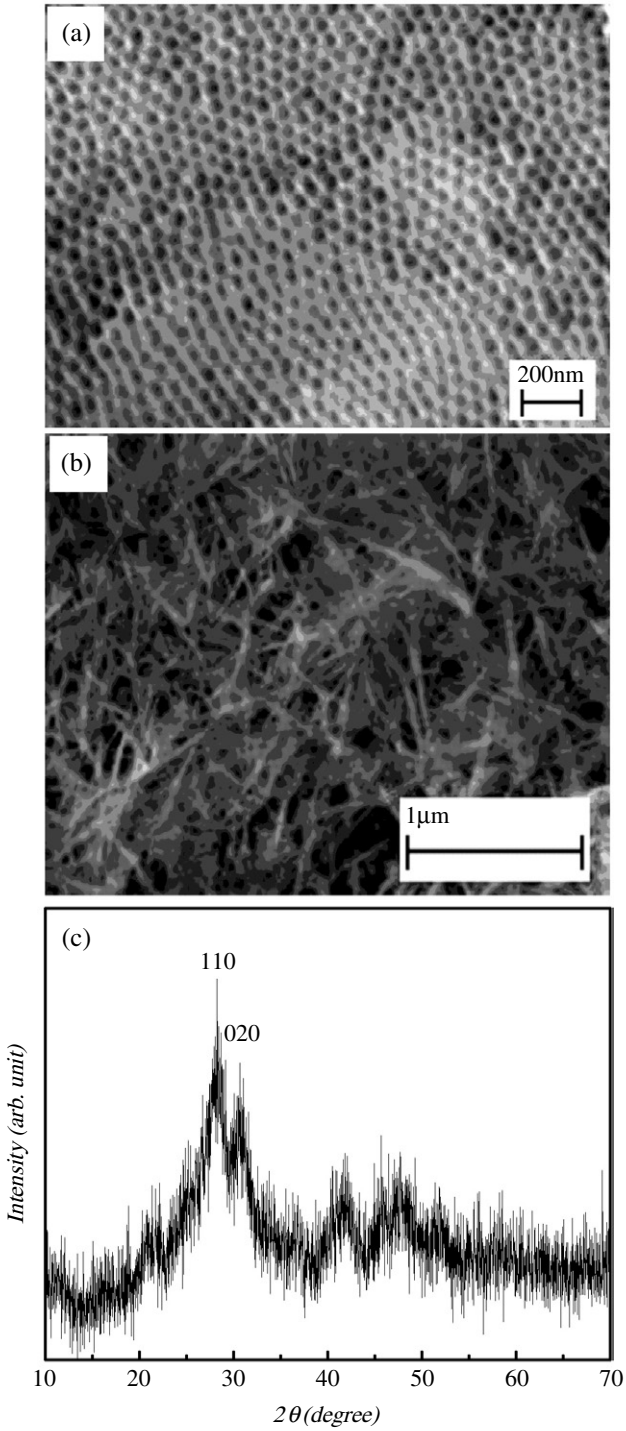

Figure 1. (a) SEM image of the AAO template, (b) SEM image of LSMO nanowires, (c) XRD pattern of LSMO nanowires.

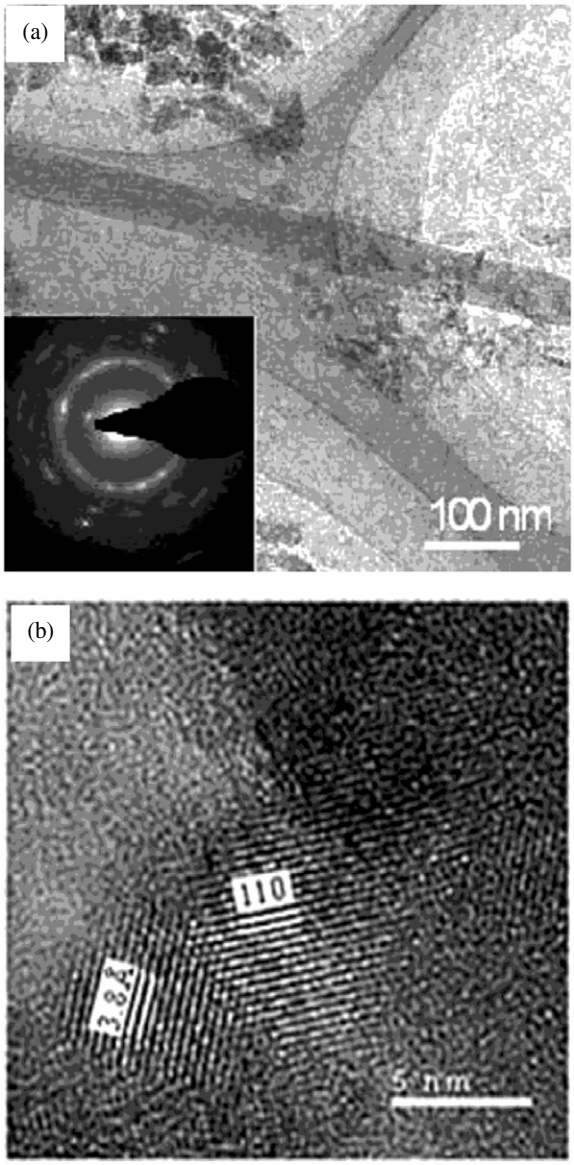

Figure 2. (a) TEM image of an isolated LSMO nanowire together with the SAED pattern (inset), and (b) HRTEM image of the cross-sectional view of the nanowire.

competing phases from coarsening [10, 13]. It is very different from the sub-micrometre-scale PS caused by quench disorder, which is considered as the intrinsic nature in bulk materials [14, 15].

When the LSMO nanowires first experienced a field-cool down to 5 K under a magnetic field of 2.0 T, the measured M (under a field of 100 Oe) as a function of T in the heating path was as given in figure 3(a). The measured M is about four times larger than that for the sample cooled under zero field. Because of the much larger length-to-diameter ratio ($\sim$200), it is expected that the effective magnetic field along the wire axis is much larger than that

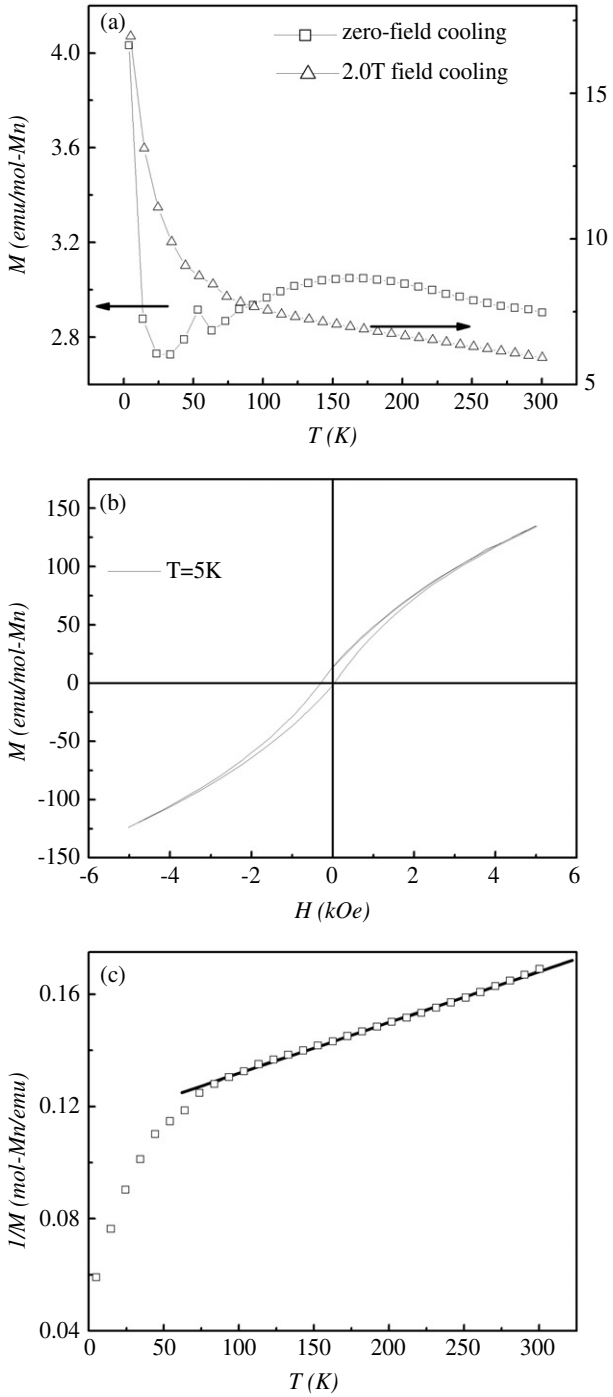

Figure 3. (a) Measured magnetization M as a function of temperature T in a heating path for LSMO nanowires after zero-field cooling and cooling under a magnetic field of 2.0 T, respectively; (b) measured magnetic field H dependence of magnetization M at 5 K for LSMO nanowires after zero-field cooling; and (c) reciprocal magnetization $(1/M)$ as a function of T for LSMO nanowires after cooling under a magnetic field of 2.0 T.

perpendicular to the wire axis. The magnetic domain will be directionally ordered after cooling the sample under a field of 2.0 T. Therefore, the value of M is higher. It seems that a field of 2.0 T is strong enough to suppress the long-range AFM state as the ground state. Because no long-range FM ordering as the ground state is favoured in the present sample, the magnetic behaviour is essentially dominated by the SPM state over the low T range. It is therefore demonstrated that the LSMO nanowire exhibits essentially different magnetic property from the ceramic or single-crystal samples.

To explain this SPM-dominant behaviour in the low T range, one may argue that the ground state for LSMO nanowires is the AFM state inside the nanowires and the spin-glass state on the surface layer. The spin-glass state on the surface plays an important role at low T because the nanowires have large surface/volume ratio, and its freezing temperature can be very low, while the PM–AFM transition point is as high as 150 K. When the M–T curve was measured in the heating path after the sample was zero-field cooled, the frozen surface spin-glass state was melted with increasing T, leading to a rapid decrease of M. Subsequently, the AFM–PM transitions proceed at the Néel point, as shown in figure 3(a). Under a 2.0 T field cooling of the nanowires, the spin-glass state becomes predominant while the AFM phase is suppressed completely, resulting in an SPM relaxation behaviour over the whole T range. The M–H loop, where H is the magnetic field, measured at 5 K and shown in figure 3(b), also indicates the SPM behaviour. In figure 3(c), the reciprocal of magnetization is plotted as a function of T, where the straight line is a fitting following the Curie–Weiss law, $M \sim C/(T - T_c)$, which produces a physically meaningless negative T_c and the freezing temperature of ∼60 K for the SPM state.

What should be noted here is that the results shown in figure 3(a) exclude any identifiable FM interaction between two neighbouring nanowires, as evidenced earlier [16]. In fact, previous reports presented similar SPM behaviours in $La_{2/3}Ca_{1/3}MnO_3$ nanodots in the range of 10–15 nm and Fe nanowires about 5 nm in diameter, where the SPM state is always dominant at low T due to the nanoscale size effect and low dimensionality [17, 18].

The PL spectra of the LSMO nanowires were measured using a visible–ultraviolet spectrophotometer at room temperature. The sample for the PL measurement was prepared by dissolving the AAO templates filled with the nanowires in 4 M NaOH solution, dispersing the LSMO nanowires in ethyl ethanol by ultrasonic vibration. The continuum spectrum of the excitation source is presented in figure 4(a) with two distinctive peaks located at 360 and 380 nm. The 360 nm wavelength is the best excitation wavelength to our sample and employed here. The measured PL spectrum is shown in figure 4(b). Significant PL signal was recorded within the wavelength range of 380–500 nm, which seems to be a combination of three PL bands. We employed the multi-peaked Gaussian fitting to the mixed band and the perfectly fitted results are plotted in figure 4(b) too.

It is found that the three PL bands are respectively located at about 400, 420 and 448 nm. It is understood that the PL spectra of LSMO materials are attributed to the following physical origins: the self-trapped excitons, the oxygen vacancies and surface states. The $La_{1-x}Sr_xMnO_3$ ($x = 0.0$–0.3) has a notable optical excitation of ∼3.0 eV [19] because of the self-trapped excitons localized on MnO_6 octahedra, which is responsible for the PL peaked at 400 nm (3.1 eV). In addition, the nanowires have a huge ratio of surface area to volume, which favours pre-evaporation of oxygen during the sintering process. Most of the surface states are oxygen vacancies or other cations adjacent to oxygen vacancies. The excitation energy on the surface would be lower than the self-trapped excitons. Therefore, it is reasonable to assign the PL band peaked at 420 nm to the excitons associated with oxygen vacancies on the surface of the LSMO nanowires. This PL band has the most intensive emission with respect to the other two, indicating the predominant role of the surface defect (vacancy) state in the

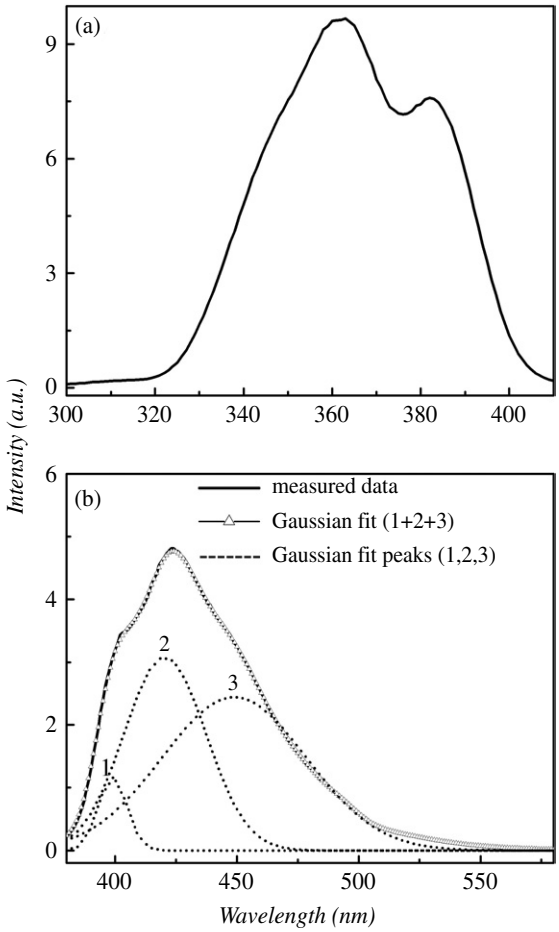

Figure 4. (a) Continuum source spectrum for PL excitation; (b) measured PL spectrum of LSMO nanowires with three bands peaked at 400, 420 and 448 nm, respectively.

LSMO nanowires. With respect to PL band 3 peaked at 448 nm, it may be caused by the residual AAO templates which take very scattered particles of small size, which were formed in the corrosion process in 4 M NaOH solution. This broad PL profile attributed to the AAO templates themselves was reported earlier [20], and our experiments revealed that its pattern may change from sample to sample, depending on the corrosion process, while the other two bands (bands 1 and 2) keep essentially the same. Along this line, further work is definitely necessary to understand the details of the PL mechanism in the LSMO nanowires.

In conclusion, we have fabricated the LSMO ($x = 0.175$) nanowires using a sol–gel AAO template method. The as-prepared nanowires show a polycrystalline perovskite structure with the diameter the same as the pore diameter of the template. The typical dimensions of the nanowires are 50 nm in diameter and tens of micrometres in length. It has been identified that the ground state of the LSMO nanowires is dominated by the AFM state at high temperature, but favours the SPM state at low temperature due to the nanoscale and low dimensionality of the nanowires. The PL spectra have been found to exhibit two bands peaked at 400 and 420 nm, which are attributed to self-trapped excitons, oxygen vacancies and surface states, respectively.

This work was supported by the National Natural Science Foundation of China through the Overseas Outstanding Younger Investigator Project (ZFR) and normal projects (50332020, 10021001, 10494037), the National Key Projects for Basic Research of China (2002CB613303, 2004CB619004) and the LSSMS of Nanjing University (M041908).

References

[1] Iijima S 1991 *Nature* **354** 56
[2] Li Y B, Bando Y, Sato T and Kurashima K 2002 *Appl. Phys. Lett.* **81** 144
[3] Yun W S, Urban J J, Gu Q and Park H 2002 *Nano Lett.* **2** 447
[4] Zhang X Y, Zhao X, Lai C W, Wang J, Tang X G and Dai J Y 2004 *Appl. Phys. Lett.* **85** 4190
[5] Shankar K S, Kar S, Raychaudhun A K and Subbanna G N 2004 *Appl. Phys. Lett.* **84** 993
[6] Martin C R 1994 *Science* **266** 1961
[7] Shankar K S and Raychaudhuri A K 2004 *Nanotechnology* **15** 1312
[8] Alexandrov A S and Bratkovsky A M 1998 *Phys. Rev. Lett.* **82** 141
[9] Ignatov A Yu, Ali N and Khalid S 2001 *Phys. Rev.* B **64** 014413
[10] Tokura Y, Urushibara A, Moritomo Y, Arima T, Asamitsu A, Kido G and Furukawa N 1994 *J. Phys. Soc. Japan* **63** 3931
Dagotto E, Hotta T and Moreo A 2001 *Phys. Rep.* **344** 1
[11] Urushibara A, Moritomo Y, Arima T, Asamitsu A, Kido G and Tokura Y 1995 *Phys. Rev.* B **51** 14103
[12] Park J H, Vescovo E, Kim H J, Kwon C, Ramesh R and Venkatesan T 1998 *Nature* **392** 794
[13] Moreo A, Yunoki S and Dagotto E 1999 *Science* **283** 2034
[14] Uehara M, Mori S, Chen C H and Cheong S-W 1999 *Nature* **399** 560
[15] Tokunaga M, Tokunaga Y and Tamegai T 2004 *Phys. Rev. Lett.* **93** 037203
[16] Chantrell R W, Walmsley N S, Gore J and Maylin M 1999 *J. Appl. Phys.* **85** 4340
[17] Katiyar P, Kumar D, Nath T K, Kvit A V, Narayan J, Chattopadhyay S, Gilmore W M, Coleman S, Lee C B, Sankar J and Singh R K 2001 *Appl. Phys. Lett.* **79** 1327
[18] Zhang X Y, Wen G H, Chan Y F, Zheng R K, Zhang X X and Wang N 2003 *Appl. Phys. Lett.* **83** 3341
[19] Shi M, Falub M C, Willmott P R, Krempasky J, Herger R, Hricovini K and Patthey L 2004 *Phys. Rev.* B **70** 140407
[20] Mei Y F, Li Z M, Chu R M, Tang Z K, Siu G G, Fu R K Y, Chu P K, Wu W W and Cheah K W 2005 *Appl. Phys. Lett.* **86** 021111